Comparison of Fontan surgical options for patients with apicocaval juxtaposition

Zhenglun Alan Wei[1], **Camille Johnson**[1], **Phillip Trusty**[1], **Morgan Stephens**[1], **Wenjun Wu**[1], **Ritchie Sharon**[2], **Balaji Srimurugan**[2], **Brijesh P. Kottayil**[2], **Sunil GS**[2], **Mark A. Fogel**[3], **Ajit P. Yoganathan**[1], **Mahesh Kappanayil**[2]

[1]Department of Biomedical Engineering, Georgia Institute of Technology, Atlanta, GA, USA

[2]Amrita Institute of Medical Sciences and Research Centre, India

[3]Children's Hospital of Philadelphia, Philadelphia, PA, USA

Abstract

Apicocaval juxtaposition (ACJ) is a rare form of viscerocardiac malpositions in association with single-ventricle congenital heart defects. The Fontan surgery is the common palliation, and possible surgical options include ipsilateral, contralateral, and intra-atrial conduits. Concerns include lower hemodynamic performances or risks of conduit compression by the cardiac mass. This study investigates the hemodynamics and clinical outcomes of ACJ patients and potential surgical improvements. Ten consecutive ACJ patients were included, along with a reference cohort of ten non-ACJ patients. Magnetic resonance images were acquired at 6 ± 0.6 year follow-up for anatomical analysis and hemodynamic assessments using computational fluid dynamics. Metrics of interest are deformation index (DI), indexed power loss (iPL), and hepatic flow distribution (HFD_{off}). A "virtual" surgery was performed to explore potential hemodynamic improvements using a straightened conduit. DI for ACJ patients fell within the DI range of non-ACJ patients. Contralateral conduits had insignificantly higher iPL (0.070 [0.032,0.137]) than ipsilateral conduits (0.041 [0.013,0.095]) and non-ACJ conduits (0.034 [0.011,0.061]). HFD_{off} was similar for the ipsilateral (21 [12,35]), contralateral (26 [7,41]), and non-ACJ Fontan conduits (17 [0,48]). Virtual surgery demonstrated that a straightened conduit reduced HFD_{off} and iPL for the contralateral and ipsilateral conduits, potentially leading to improved clinical outcomes. In this limited sample, the hemodynamic performance of ACJ patients was not significantly different from their non-ACJ counterparts. The use of a straightened conduit option could potentially

Compliance with Ethical Standards

Conflict of Interest: All authors declare that they have no conflict of interest.

Ethical approval: All procedures performed in studies involving human participants were complied with the Institutional Review Boards of the participating institutions: Georgia Institute of Technology and Children's Hospital of Philadelphia (IRB Number H05236, Understanding/Improving Fontan Flow Dynamics II) and with the 1964 Helsinki declaration and its later amendments or comparable ethical standards. This article does not contain any studies with animals performed by any of the authors.

Informed consent: Informed consent was obtained from all individual participants included in the study.

improve patient outcomes. Additionally, the fear of significant compression of conduits for ACJ patients was unsupported.

Keywords

Computational Fluid Dynamics; Fontan; Apicocaval Juxtaposition

Introduction

The Fontan procedure is a common treatment for patients with functional single ventricle defects. This three-stage procedure results in a total cava-pulmonary connection (TCPC), connecting the systemic venous return to pulmonary circulations by circumventing the sub-pulmonary ventricle. There are currently two primary approaches to construct the TCPC: intra-atrial (IA) shunt or an extra-cardiac (EC) shunt. An IA shunt utilizes part of the atrium to construct the TCPC and has the potential for growth. Unfortunately, patients with an IA shunt may suffer from a significantly higher incidence of arrhythmias than their EC counterparts [1]. EC shunts are synthetic, PTFE conduits with advantages in the ease of surgery, often without aortic cross-clamping and less atrial suturing [2]. Previous studies also suggest the advantage of rhythm stabilization of EC shunt compensates for its disadvantage of a non-growing prosthetic tube [3].

In cardiac malposition where there is apicocaval juxtaposition (ACJ), it becomes technically difficult to construct the standard EC shunt because of the blockage of cardiac mass in the straight path between the inferior vena cava (IVC) and superior vena cava (SVC). ACJ is a viscerocardiac malposition resulting in the cardiac apex pointing towards the same side as IVC, as shown in Fig. 1. Therefore, forms of the EC shunt for ACJ patients include (1) ipsilateral conduit, where a shunt connects the IVC to the ipsilateral branch of the pulmonary arteries (PAs), passing behind the cardiac mass (Fig. 2a), and (2) contralateral conduit, where a shunt connects the IVC to the contralateral branch of the PAs (Fig. 2b).

These two options have inherent disadvantages. The ipsilateral conduit passes behind the cardiac mass as shown; therefore, it may be subject to physical compression during diastole. The contralateral conduit is less invasive and not associated with conduit compression. However, it has a long, curved path crossing the spine which may be susceptible to kinking [4,5].

Similar to regular Fontan patients, ACJ patients may suffer from long-term complications. Examples are limited exercise capacity and risks of pulmonary arteriovenous malformation (PAVM), which are linked to poor TCPC hemodynamics [6–8]. In the past decade, computational fluid dynamics (CFD) has become a reliable tool to assess TCPC hemodynamics [9–11]. Menon *et al.* [12] conducted a virtual surgery study for an ACJ patient and compared the performance of a contralateral conduit and an IA shunt. The study showed that the long conduit of the contralateral option resulted in increased power loss inside the Fontan conduit. However, greater power loss caused by the collision of the IVC and SVC flows is avoided by their offset. Accordingly, the net power loss of the TCPC with the contralateral conduit is lower than that with the IA shunt. The same group later

performed a computational study with a larger cohort and observed no clinically significant differences in net power loss between the two types of EC shunts and the IA shunt [13]. Additionally, they observed one patient with a kinked contralateral conduit and found that kinking significantly increased power loss.

Though they compared the hemodynamic differences among surgical options for ACJ patients, previous studies marginally assessed the performance of these options based on clinically relevant hemodynamic metrics, including indexed power loss (iPL) and hepatic flow distribution (HFD). Though similar to power loss used in previous studies related to ACJ patients [13,12], iPL has been emphasized by recent papers as an important factor in indicating exercise capacity [14] and quality of life [15] of Fontan patients. In addition, unbalanced HFD may lead to the progression of PAVMs [16–18], and it is sensitive to the offset of IVC and SVC [19].

This study enrolled ten ACJ patients (7 ipsilateral and 3 contralateral conduits) and an additional ten non-ACJ patients as a reference group. Clinical outcomes were reported for ACJ patients. Computational fluid dynamic simulations were used to calculate iPL and HFD for each patient, which were then compared across conduit types as well as with the reference group. Time-varying cross-sectional areas of the Fontan conduit were analyzed to quantify the compression of the conduits from the cardiac mass. To capitalize on the available patient data, an in-house virtual surgery platform was also used to generate a straightened conduit (possibly an IA shunt) for ACJ patients, and simulations were conducted to explore potential hemodynamic improvements by using this virtual surgical option.

Material and Methods

Patient Cohort

Ten consecutive ACJ patients who underwent Fontan completion at Amrita Institute of Medical Sciences, Kochi, India, during the study period were included in the study (Table 1). Seven patients were strictly suited only for the single ventricle pathway of repair. Three patients with congenitally corrected transposition of great arteries (CCTGA) were anatomically suitable for potential biventricular repair but were subjected to the Fontan pathway owing to technical and socio-economic barriers in attempting a complex biventricular repair. It is not uncommon for complex biventricular repair candidates to be diverted to the single-ventricle pathway in resource-limited environments [20]. The median age at Fontan was 10 years, and the median intervening interval was 8 years. In most cases, the delay in surgery was due to the anticipated technical challenges in Fontan operation in ACJ. Hemodynamic and anatomical suitability for Fontan operation was ascertained and confirmed through a comprehensive preoperative assessment that included echocardiography, cardiac catheterization, and cardiac magnetic resonance (MR) imaging or computed tomography (CT). There were specific concerns regarding Fontan surgery at older ages (five patients were older than 10 years, two of whom were over 20 years of age); the patients and their families were counseled accordingly. Informed consent was obtained from all patients, and all study protocols complied with the Institutional Review Boards of the participating institutions.

Additionally, ten patients without ACJ from the Georgia Tech Fontan database were chosen as a reference cohort. Patients were selected to best match body surface area (BSA) and age (Fig. 3).

Surgical Details

All surgeries were performed on cardiopulmonary bypass. The final decision for the site of conduit placement was made 'on the operating table' after thorough completion of the dissection, which entailed

1. completely freeing the cardiac apex off adhesions;

2. completely exposing the plane between the posterior aspect of the ventricular mass and the posterior pericardium till the pulmonary veins entering the atrium were seen;

3. detaching the right atrial wall from the pericardium and exposing the Glenn circuit;

4. dissecting the branch pulmonary artery to pulmonary artery confluence;

5. mobilizing the IVC off its adhesions.

A stay suture taken at the apex with gentle retraction and looping of the IVC enabled the surgeon to understand the extent of the ACJ and to thoroughly explore the possibility of placing the conduit between the IVC and the ipsilateral branch pulmonary artery. An important consideration of planning the lie of the conduit was to avoid potential compression of the ipsilateral pulmonary veins by the Fontan conduit. Towards this purpose, pulmonary veins were dissected as much as possible towards the hilum, to potentially allow them to fall posteriorly and avoid compression by the anteriorly placed conduit (in the ipsilateral approach).

The possibility of anastomosing the Fontan conduit to the contralateral branch pulmonary artery, crossing the spine, was considered as an alternative approach only when an ipsilateral anastomosis appeared unfeasible or risky. While technically, the contralateral approach would have been possible in all the cases, there was strong surgeon perception that the longer length of the conduit in this approach, with greater potential for kinking along the course, and the adherence of the left atrial appendage to the undersurface of the morphological left pulmonary artery in extreme dextroverted hearts – would all make this an anatomically and hemodynamically inferior option as compared to a shorter, straighter ipsilateral conduit. There was however no data to substantiate or refute this perception. The contralateral anastomosis was done in only three patients. The IA Shunt approaches were not considered

Six of ten were selectively operated under normothermic, cardioplegic arrest because they either need significant manipulation of the heart during dissection and anastomosis or showed subtle signs of hemodynamic instability during the dissection. This was believed to make the myocardium less irritable and allowed for the heart to better accommodate to its new premise with a prosthetic conduit placed behind it.

MRI Data Acquisition Protocol

MR imaging was done for all patients, (median interval of 3 years after Fontan completion) on Signa HDxT 1.5 Tesla scanner, General Electric (GE) Healthcare. MR sequences obtained included steady-state free precession (SSFP 7 or 2D-FIESTA) with suspended breathing in orthogonal planes, gadolinium-enhanced three-dimensional angiogram, and free-breathing phase-contrast sequences. Patient-specific anatomies were reconstructed using InVesalius (https://www.cti.gov.br/pt-br/invesalius). Geomagic Studio (Geomagic Inc, NC, USA) was used to fit a 3D surface that is suitable for further mesh generation for numerical simulations. Patient-specific, time-averaged blood flow rates were obtained by segmenting through-plane velocities from phase-contrast magnetic resonance imaging by using the freely available software Segment (http://segment.heiberg.se) [21].

The cross-sectional areas (Fig. 4) of the Fontan conduit were obtained from cine cardiac MR images, which usually have 9–10 slices/planes along the Fontan conduit and 16~20 time points over a cardiac cycle. A deformation index (DI) of the conduit was calculated:

$$DI = \frac{A(t)_{\max} - A(t)_{\min}}{A(t)_{avg}}$$ (1)

where $A(t)_{max}$, $A(t)_{min}$, and $A(t)_{avg}$ are the maximum, minimum, and time-averaged value of conduit cross-sectional areas over one cardiac cycle.

Computational Fluid Dynamics

Image-based CFD simulation is a cost-effective, non-invasive approach to obtain high-resolution biophysical parameters for Fontan patients. In this study, unsteady CFD simulations were executed using ANSYS Fluent 17.0 (ANSYS, Inc., Canonsburg, PA). Polyhedral meshes were made by converting unstructured tetrahedral meshes generated in ANSYS Workbench Meshing Module (ANSYS, Inc., Canonsburg, PA). A mesh independence study conducted in a previous study indicated that an adequate mesh size is $D_{avg}/20$, where D_{avg} is the average diameter of all TCPC inlets and outlets [22]. Additionally, a boundary layer zone with three layers of boundary mesh ([$D_{avg}/60$]×3) was created to improve numerical accuracy near the walls. The setups for the simulation domain, boundary conditions, and flow solver have detailed in Wei et al. [23].

Hemodynamic Metrics

The CFD simulations resulted in high-fidelity velocity and pressure fields from which iPL and HFD were calculated. HFD was defined by the percentage of IVC flow to the left pulmonary artery. Since 50% HFD is usually considered ideal, $HFD_{off} = |HFD-50\%|$ is defined to describe the deviation from the balanced distribution. Power loss is defined as

$$PL = \int_{Inlets + Outlets} \left(p + \tfrac{1}{2}\rho v^2\right)v \cdot dA$$ (2)

where ρ, p, v, and A are blood density, static pressure, velocity, and vessel area, respectively. HFD and PL were averaged over one cardiac cycle after the solution became periodically stable. Indexed power loss (iPL) was further defined as follows:

$$\text{iPL} = \frac{\overline{\text{PL}}}{\rho \overline{Q_s}^3 / \text{BSA}^2}$$

(3)

where $\overline{Q_s}$ is time-averaged systemic venous flow and $\overline{\text{PL}}$ is the time-averaged PL.

Virtual Surgery

Virtual surgery was performed in SURGEM III [24,25] by straightening the conduit while keeping the anastomosis location between the Fontan conduit and pulmonary arteries the same, as shown in Fig. 5. This virtual surgery platform has been used to successfully optimize surgical strategies for Fontan patients [26].

The difference in simulated metrics between the straightened and original conduits was calculated as:

$$\Delta iPL = \left(iPL_{straightened} - iPL_{original} \right) / iPL_{original}$$

(4)

and

$$\Delta HFD_{OFF} = \left(HFD_{straightened} - HFD_{original} \right) / HFD_{original}$$

(5)

Statistical Analysis

All variables are presented as mean values [minimum values, maximum value] unless otherwise stated. IBM SPSS Statistics (IBM, Inc., Aramark, NY) was used to perform statistical analyses. Normality was checked using the Shapiro-Wilk test. Bivariate correlations were analyzed using either Spearmen's or Pearson's correlation test for non-normally or normally distributed data, respectively. In all comparisons, a p-value<0.05 was considered significant.

Results

Clinical Outcomes

The median duration of postoperative hospital stay was 15.5 days (range 13–27 days; mean 16.7 days). Two patients had persistent pleural effusion requiring more than one week of intercostal tube drainage. There were no other notable morbidities during the immediate post-operative period.

Intermediate outcomes were evaluated by a follow-up of 6 [5.2–7] years since the Fontan. All patients continued on regular follow-up with periodic clinical exams, echocardiogram, electrocardiogram, exercise tests, liver function tests, and prothrombin time tests. Two patients had episodes of supraventricular tachycardia and were treated with maintenance doses of oral beta-blockers. Four patients were on oral anticoagulation (Warfarin), with a

target International Normalized Ratio (INR) of 2–2.5, and six patients were maintained on an antiplatelet agent (Aspirin) only. One patient completed her pregnancy three years after the Fontan surgery. None of the patients showed any clinical or laboratory signs of Fontan dysfunction or maladaptation during this period of follow-up.

Deformation Index and Compression

Figure 6 illustrates the DI for all ACJ patients along with the range of DI for non-ACJ patients. DIs of non-ACJ patients were obtained from PC-MRI, which usually have one or two planes along the Fontan conduit. Therefore, only a range of DIs was reported for non-ACJ patients, and the range is 16–28%, as indicated in Fig. 6. Additionally, the cardiac MR images revealed evidence of mild compression of the ipsilateral lower pulmonary veins by the Fontan conduit in five patients, as shown in Table 2. Pulmonary vein compression only occurred in patients with an ipsilateral conduit and was limited to the lower pulmonary veins.

Comparison of Hemodynamic Performances

Figure 7 illustrates comparisons of the iPL and HFD_{off} between ipsilateral and contralateral conduits, as well as the reference group. The iPL for contralateral conduits (0.070 [0.032,0.137]) is higher than that for ipsilateral conduits (0.041 [0.013,0.095]) and non-ACJ conduits (0.034 [0.011,0.061]). However, the difference is not statistically significant. Additionally, no statistical difference was observed in HFD_{off} between ipsilateral, contralateral, and non-ACJ Fontan conduits (21 [12,35], 26 [7,41], and 17 [0,48], respectively)

Possible Improvements

The straightened conduit was created for two patients with a contralateral conduit and the other two with an ipsilateral conduit. The simulated results show that the straightened option lowers 3.4 [2.5, 4.3] for HFD_{off} and 1.6 [−1.0, 4.2] for iPL regarding the ipsilateral conduit, and decreases 0.8 [−5.5, 3.9] for HFD_{off} and 12.0 [10.9, 13.2] for iPL from the original contralateral conduits.

Discussion

The relative rarity of the morphology, lack of data on surgical outcomes, and fear of suboptimal hemodynamic performance due to the unusual conduit position often lead to deferring of the surgical decision in ACJ patients. Previous studies on ACJ are scarce [27,5,13,12,28–31], and there is a lack of consensus on the optimal treatment for ACJ patients. While a perceived fear exists regarding dynamic compression of the conduit by the heart mass in the ipsilateral option and concern regarding elevated power loss in the contralateral option, the IA shunt is associated with a higher risk of atrial arrhythmias. Therefore, both decisions have disadvantages, and the choice is often made based on the surgeon's experience and technical expertise.

This study demonstrated that, in the present cohort, neither the ipsilateral nor contralateral conduits expressed significantly more deformation than non-ACJ Fontan conduits. This is

the first evidence to show that the ipsilateral conduit is not remarkably compressed by the cardiac mass. Though mild compression of the ipsilateral lower pulmonary veins was observed in patients with ipsilateral Fontan conduit, no clinical manifestations resulting from this compression are evident yet in these patients. Nevertheless, special attention is merited for these patients to monitor possible long-term complications.

Furthermore, this study demonstrated that no significant difference exists in iPL between ACJ patients with EC options and non-ACJ patients. The range of iPL for contralateral conduits is larger than that of ipsilateral conduits, suggesting that patients with a contralateral conduit may be prone to lower exercise capacity [12,13]. This study also showed that contralateral conduits have higher cohort-averaged HFD_{off} than the ipsilateral shunts. However, this difference was relatively small and would likely not result in any differences in clinical outcomes.

Additionally, the virtual surgery study shows that a straightened option reduces both the HFD_{off} and iPL for patients with a contralateral conduit, while the straightened option only slightly enhanced the hemodynamic performance for patients with an ipsilateral conduit. This finding suggests that the contralateral conduit may not be the optimal option for ACJ patients and that a straightened conduit could result in a better hemodynamic performance. Therefore, the straightened option should be considered for certain patients, e.g. in surgical planning procedure, which may translate into better hemodynamics. In comparison with the simple straightened option examined in this study, an IA shunt can further reduce the length of the Fontan conduit and the offset between the conduit and SVC, which could lead to additional reductions in terms of iPL and HFD_{off} [14,19]. Therefore, the IA shunt may be included as an option for optimal TCPC performance in hemodynamics, especially for those patients who are only suitable for contralateral conduits. It is worth noting that this study only demonstrates the hemodynamic advantages of the straightened option or the IA shunt. However, the choice of the IA shunt should be made only after deliberately weighing the hemodynamic performance and surgical feasibility and risks.

The authors acknowledge several limitations to this study. First, the current study involves a small cohort like most previous studies [31,30,29,28,27], majorly because of the rarity of the AJC patients. Long-term follow-up data on this rare subset of patients would be an important area for future research. Secondly, the CFD utilized flow data under breath-held conditions to obtain simulated hemodynamic metrics, while long-term hemodynamic effects occur under free-breathing conditions [32]. However, the effect of anatomical differences between surgical options should overwhelm the influence of using flow data under breath-held conditions[33,34]. Last, the simulations utilized the assumption of a rigid wall. Previous studies have demonstrated that the wall deformation for non-ACJ conduits does not considerably affect the iPL and HFD obtained from CFD simulation [35,36]. It is, therefore, reasonable to adopt this assumption for ACJ patients as this study demonstrated non-significant vessel deformation between ACJ and non-ACJ Fontan conduits.

This study adds to the limited knowledge of Fontan surgical options for ACJ patients. The decision to operate on these patients need not be delayed or offset by apprehensions regarding the compression of the Fontan conduit by the cardiac mass. CFD data and the

Author Manuscript

clinical follow-up on the patients in this cohort shows that it is possible to achieve good technical and hemodynamic results from Fontan operation even in these complex defects. The study also emphasizes that hemodynamic efficiency of the Fontan circuit in these patients may be optimized through the better understanding of hemodynamics, and utilization of CFD and surgical planning. The best surgical approach may need to be tailored to patient-specific anatomy and physiology.

Acknowledgments

Reference

1. Li D, Fan Q, Hirata Y, Ono M, An Q (2017) Arrhythmias After Fontan Operation with Intra-atrial Lateral Tunnel Versus Extra-cardiac Conduit: A Systematic Review and Meta-analysis. Pediatr Cardiol 38 (4):873–880. doi:10.1007/s00246-017-1595-8 [PubMed: 28271152]

2. Katogi T (2012) Extracardiac conduit Fontan procedure versus intra-atrial lateral tunnel Fontan procedure. Gen Thorac Cardiovasc Surg 60 (12):792–795. doi:10.1007/s11748-012-0161-9 [PubMed: 23229999]

3. Ochiai Y, Imoto Y, Sakamoto M, Kajiwara T, Sese A, Watanabe M, Ohno T, Joo K (2009) Mid-term follow-up of the status of Gore-Tex graft after extracardiac conduit Fontan procedure. Eur J Cardiothorac Surg 36 (1):63–67; discussion 67–68. doi:10.1016/j.ejcts.2009.02.013 [PubMed: 19329333]

4. de Leval MR (2013) Re: Total cavopulmonary connection in patients with apicocaval juxtaposition: optimal conduit route using preoperative angiogram and flow simulation. Eur J Cardiothorac Surg 44 (1):e52. doi:10.1093/ejcts/ezt170 [PubMed: 23575943]

5. Gil-Jaurena JM, Perez-Caballero R, Pita A, Gonzalez-Lopez M (2016) Extracardiac Fontan in apicocaval juxtaposition. Asian Cardiovasc Thorac Ann 24 (2):178–180. doi:10.1177/0218492314553613 [PubMed: 25249659]

6. Wei ZA, Trusty PM, Tree M, Haggerty CM, Tang E, Fogel M, Yoganathan AP (2017) Can time-averaged flow boundary conditions be used to meet the clinical timeline for Fontan surgical planning? J Biomech 50:172–179. doi:10.1016/j.jbiomech.2016.11.025 [PubMed: 27855985]

7. Tree M, Wei ZA, Trusty PM, Raghav V, Fogel M, Maher K, Yoganathan A (2018) Using a Novel In Vitro Fontan Model and Condition-Specific Real-Time MRI Data to Examine Hemodynamic Effects of Respiration and Exercise. Annals of Biomedical Engineering 46 (1):135–147. doi:10.1007/s10439-017-1943-0 [PubMed: 29067563]

8. Rijnberg FM, Hazekamp MG, Wentzel JJ, de Koning PJH, Westenberg JJM, Jongbloed MRM, Blom NA, Roest AAW (2018) Energetics of Blood Flow in Cardiovascular Disease: Concept and Clinical Implications of Adverse Energetics in Patients With a Fontan Circulation. Circulation 137 (22):2393–2407. doi:10.1161/CIRCULATIONAHA.117.033359 [PubMed: 29844073]

9. Trusty PM, Wei Z, Rychik J, Russo PA, Surrey LF, Goldberg DJ, Fogel MA, Yoganathan AP (2018) Impact of hemodynamics and fluid energetics on liver fibrosis after Fontan operation. J Thorac Cardiovasc Surg 156 (1):267–275. doi:10.1016/j.jtcvs.2018.02.078 [PubMed: 29609888]

10. Trusty PM, Wei Z, Rychik J, Graham A, Russo PA, Surrey LF, Goldberg DJ, Yoganathan AP, Fogel MA (Accepted) Cardiac Magnetic Resonance Derived Metrics are Predictive of Liver Fibrosis in Fontan Patients. Annals of Thoracic Surgery

11. Yang W, Feinstein Ja, Shadden SC, Vignon-Clementel IE, Marsden AL (2013) Optimization of a Y-graft design for improved hepatic flow distribution in the fontan circulation. Journal of biomechanical engineering 135 (1):011002–011002. doi:10.1115/1.4023089 [PubMed: 23363213]

12. Menon PG, Yoshida M, Pekkan K (2013) Presurgical evaluation of Fontan connection options for patients with apicocaval juxtaposition using computational fluid dynamics. Artif Organs 37 (1):E1–8. doi:10.1111/j.1525-1594.2012.01555.x [PubMed: 23145982]

13. Yoshida M, Menon PG, Chrysostomou C, Pekkan K, Wearden PD, Oshima Y, Okita Y, Morell VO (2013) Total cavopulmonary connection in patients with apicocaval juxtaposition: optimal conduit route using preoperative angiogram and flow simulation. Eur J Cardiothorac Surg 44 (1):e46–52. doi:10.1093/ejcts/ezt118 [PubMed: 23530028]

14. Tang E, Wei Z, Whitehead KK, Khiabani RH, Restrepo M, Mirabella L, Bethel J, Paridon SM, Marino BS, Fogel MA, Yoganathan AP (2017) Effect of Fontan geometry on exercise haemodynamics and its potential implications. Heart 103 (22):heartjnl-2016–310855. doi:10.1136/heartjnl-2016-310855

15. Marino BS, Fogel M, Mercer-Rosa LM-R, Wei ZAW, Trusty PM, Tree M, Tang E, Restrepo M, Whitehead KK, Paridon SM, Yoganathan A (2017) Poor Fontan Geometry, Hemodynamics, and Computational Fluid Dynamics Are Associated With Worse Quality of Life. Paper presented at the Circulation, 2017-11-14 00:00:00

16. Pike NA, Vricella LA, Feinstein JA, Black MD, Reitz BA (2004) Regression of severe pulmonary arteriovenous malformations after Fontan revision and "hepatic factor" rerouting. The Annals of Thoracic Surgery 78 (2):697–699. doi:10.1016/j.athoracsur.2004.02.003 [PubMed: 15276554]

17. Trusty PM, Wei Z, Tree M, Kanter KR, Fogel MA, Yoganathan AP, Slesnick TC (2017) Local Hemodynamic Differences Between Commercially Available Y-Grafts and Traditional Fontan Baffles Under Simulated Exercise Conditions: Implications for Exercise Tolerance. Cardiovasc Eng Technol 8 (3):390–399. doi:10.1007/s13239-017-0310-5 [PubMed: 28560706]

18. Trusty PM, Wei Z, Sales M, Kanter KR, Fogel MA, Yoganathan AP, Slesnick TC (2019) Y-graft modification to the Fontan procedure: Increasingly balanced flow over time. J Thorac Cardiovasc Surg doi:10.1016/j.jtcvs.2019.06.063

19. Tang E, Restrepo M, Haggerty CM, Mirabella L, Bethel J, Whitehead KK, Fogel MA, Yoganathan AP (2014) Geometric Characterization of Patient-Specific Total Cavopulmonary Connections and its Relationship to Hemodynamics. JACC: Cardiovascular Imaging 7 (3):215–224. doi:10.1016/j.jcmg.2013.12.010 [PubMed: 24529885]

20. Kottayil BP, Sunil GS, Kappanayil M, Mohanty SH, Francis E, Vaidyanathan B, Balachandran R, Nair SG, Kumar RK (2014) Two-ventricle repair for complex congenital heart defects palliated towards single-ventricle repair. Interact Cardiovasc Thorac Surg 18 (3):266–271. doi:10.1093/icvts/ivt495 [PubMed: 24310735]

21. Heiberg E, Sjögren J, Ugander M, Carlsson M, Engblom H, Arheden H (2010) Design and validation of Segment - freely available software for cardiovascular image analysis. BMC Med Imaging 10 (1)

22. Wei ZA, Tree M, Trusty PM, Wu W, Singh-Gryzbon S, Yoganathan A (2017) The Advantages of Viscous Dissipation Rate over Simplified Power Loss as a Fontan Hemodynamic Metric. Ann Biomed Eng doi:10.1007/s10439-017-1950-1

23. Wei ZA, Huddleston C, Trusty PM, Singh-Gryzbon S, Fogel MA, Veneziani A, Yoganathan AP (2019) Analysis of Inlet Velocity Profiles in Numerical Assessment of Fontan Hemodynamics. Ann Biomed Eng doi:10.1007/s10439-019-02307-z

24. Luffel M, Sati M, Rossignac J, Yoganathan AP, Haggerty CM, Restrepo M, Slesnick TC, Kanter KR, Del Nido P, Fogel MA (2016) SURGEM: A solid modeling tool for planning and optimizing pediatric heart surgeries. CAD Computer Aided Design 70:3–12. doi:10.1016/j.cad.2015.06.018

25. Trusty PM, Slesnick TC, Wei ZA, Rossignac J, Kanter KR, Fogel MA, Yoganathan AP (2018) Fontan Surgical Planning: Previous Accomplishments, Current Challenges, and Future Directions. J Cardiovasc Transl Res 11 (2):133–144. doi:10.1007/s12265-018-9786-0 [PubMed: 29340873]

26. Trusty PM, Wei ZA, Slesnick TC, Kanter KR, Spray TL, Fogel MA, Yoganathan AP (2019) The first cohort of prospective Fontan surgical planning patients with follow-up data: How accurate is surgical planning? The Journal of Thoracic and Cardiovascular Surgery 157 (3):1146–1155. doi:10.1016/j.jtcvs.2018.11.102 [PubMed: 31264966]

27. Chen W, Lu Y, Ma L, Yang S, Xia Y, Zou M, Chen X (2018) Conduit Route Selection for Total Cavopulmonary Connection in Patients with Apicocaval Juxtaposition. Semin Thorac Cardiovasc Surg doi:10.1053/j.semtcvs.2018.07.004

28. Morizumi S, Kato H, Kanemoto S, Noma M, Abe M, Sakakibara Y, Hiramatsu Y (2012) Appropriate route selection for extracardiac total cavopulmonary connection in apicocaval juxtaposition. Ann Thorac Surg 94 (1):179–184. doi:10.1016/j.athoracsur.2012.03.026 [PubMed: 22579399]

29. Sakurai T, Kado H, Nakano T, Hinokiyama K, Oda S, Sugiura J, Ushijima T, Ueda Y (2010) The impact of extracardiac conduit-total cavopulmonary connection on apicocaval juxtaposition. Eur J Cardiothorac Surg 38 (4):439–444. doi:10.1016/j.ejcts.2010.02.032 [PubMed: 20643561]

30. Kawahira Y, Nishigaki K, Ueno T (2006) Extracardiac Fontan procedure bridging the vertebra for apico-caval juxtaposition. Ann Thorac Surg 82 (1):350–352. doi:10.1016/j.athoracsur.2005.07.059 [PubMed: 16798257]

31. Kitayama H, Oku H, Matsumoto T, Onoe M (2001) Total cavopulmonary connection using a pedicled pericardial conduit for a patient with apicocaval juxtaposition. The Annals of Thoracic Surgery 72 (4):1393–1394. doi:10.1016/s0003-4975(00)02591-1 [PubMed: 11603478]

32. Wei Z, Whitehead KK, Khiabani RH, Tree M, Tang E, Paridon SM, Fogel MA, Yoganathan AP (2016) Respiratory Effects on Fontan Circulation During Rest and Exercise Using Real-Time Cardiac Magnetic Resonance Imaging. Ann Thorac Surg 101 (5):1818–1825. doi:10.1016/j.athoracsur.2015.11.011 [PubMed: 26872728]

33. Tang E, Wei ZA, Trusty PM, Whitehead KK, Mirabella L, Veneziani A, Fogel MA, Yoganathan AP (2019) The effect of respiration-driven flow waveforms on hemodynamic metrics used in Fontan surgical planning. Journal of Biomechanics 82:87–95. doi:10.1016/j.jbiomech.2018.10.013 [PubMed: 30414631]

34. Wei Z, Trusty P, Zhang Y, Tang E, Whitehead K, Fogel M, Yoganathan A (Accepted) Is free-breathing phase-contrast MRI needed for Fontan Preintervention Planning? Journal of Cardiovascular Magnetic Resonance

35. Long CC, Hsu MCCMc, Bazilevs Y, Feinstein JA, Marsden AL (2012) Fluid – structure interaction simulations of the Fontan procedure using variable wall properties. International Journal for Numerical Methods in Biomedical Engineering 28 (January):513–527. doi:10.1002/cnm [PubMed: 25099455]

36. Mirabella L, Haggerty CM, Passerini T, Piccinelli M, Powell AJ, Del Nido PJ, Veneziani A, Yoganathan AP (2013) Treatment planning for a TCPC test case: a numerical investigation under rigid and moving wall assumptions. International journal for numerical methods in biomedical engineering 29 (2):197–216. doi:10.1002/cnm.2517 [PubMed: 23345252]
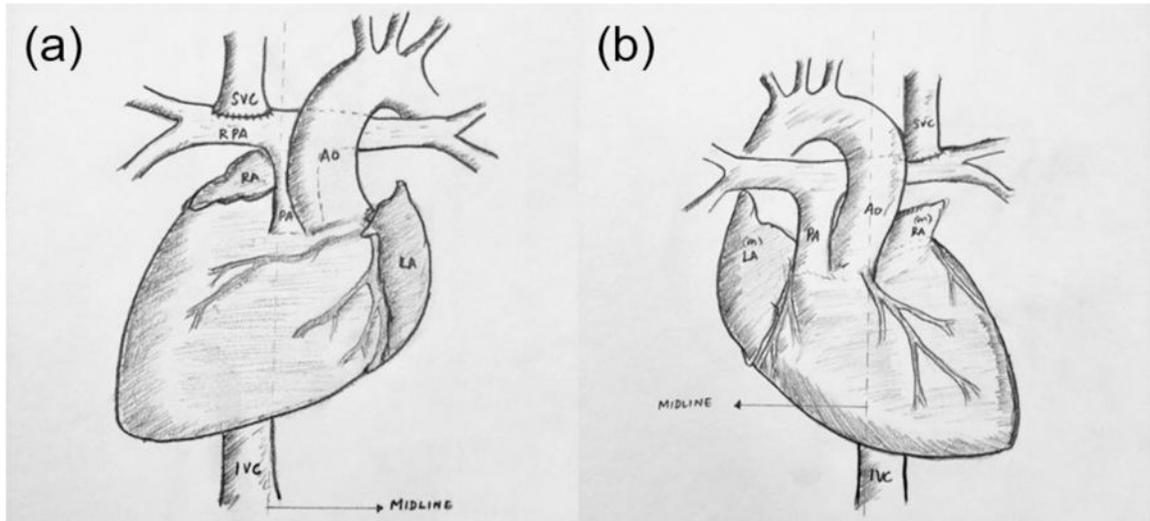
Figure 1.
Typical anatomy of ACJ patients: (a) situs solitus with dextrocardia and (b) situs inversus with levocardia.
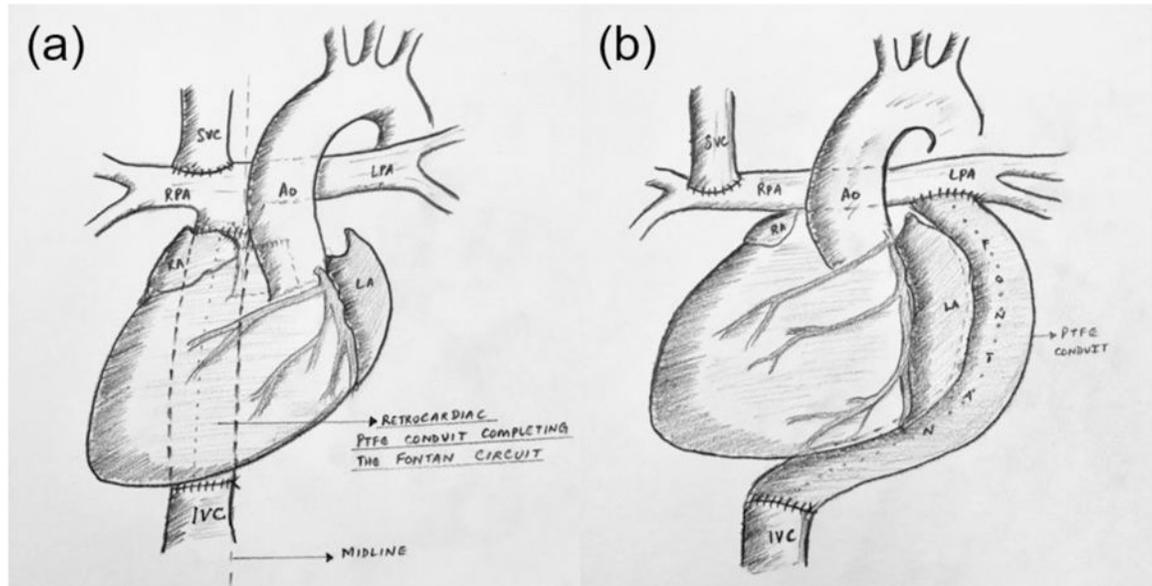
Figure 2.
Options of EC shunt for ACJ patients: (a) ipsilateral shunt and (b) contralateral shunt. The images drawn in this figure is based on the anatomy of situs solitus with dextrocardia.
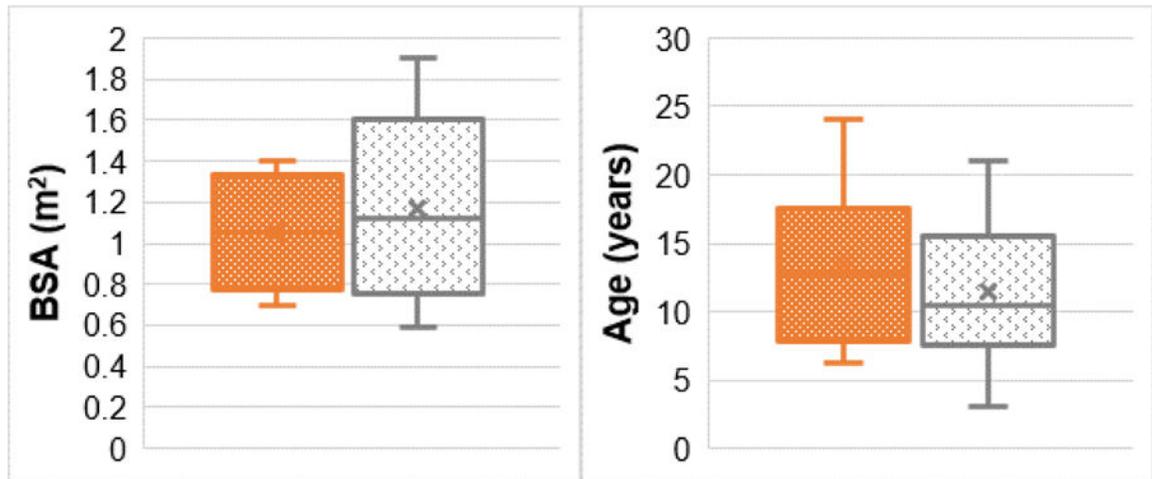
Figure 3.
Box and Whisker plots for ACJ patients (orange) and the control group (non-ACJ patients with a regular Fontan conduit, gray).
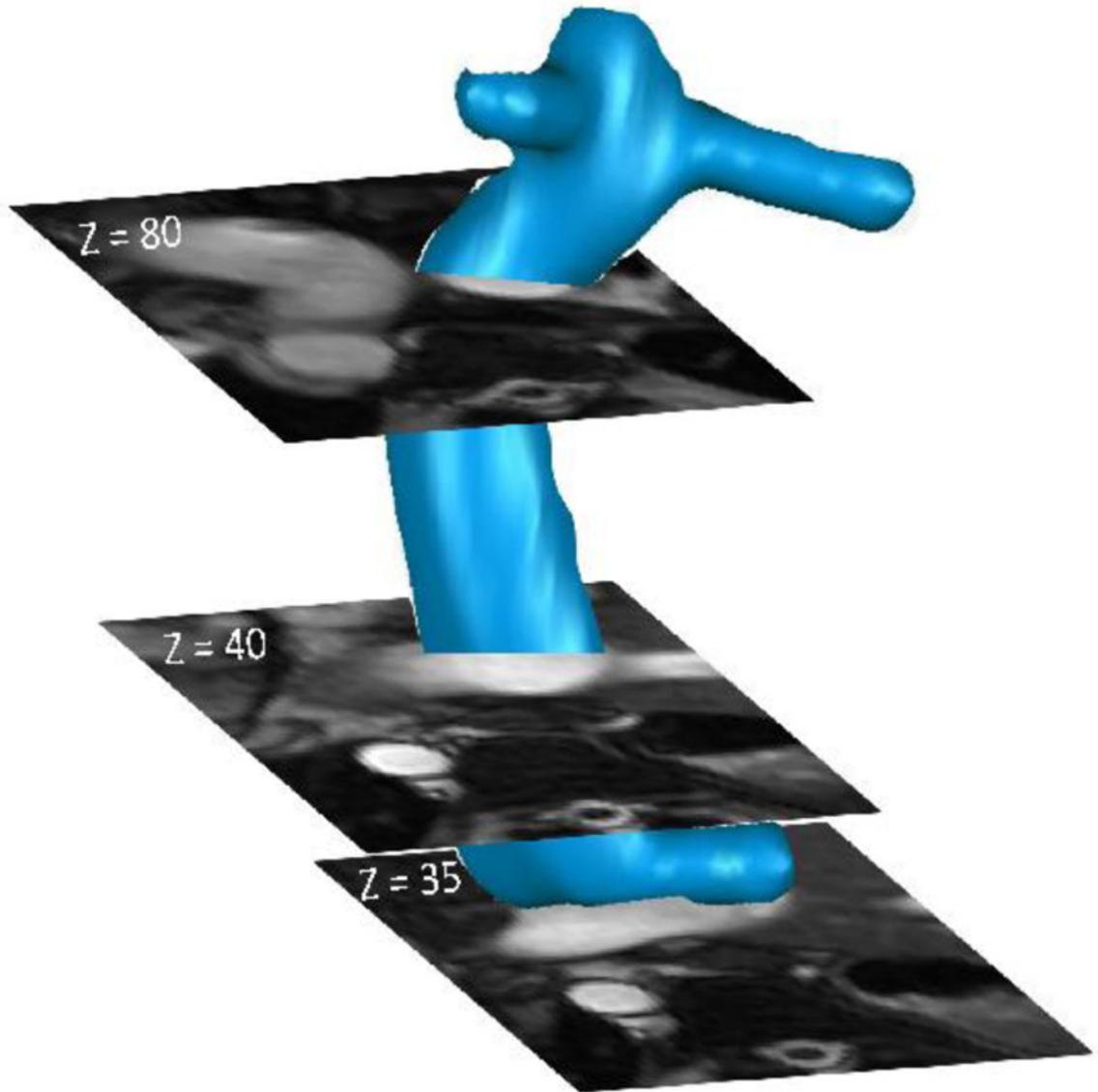
Figure 4.
A illustration of planes for phase-contrast MRI acquisition

Original Conduit

Straightened Option

Ipsilateral
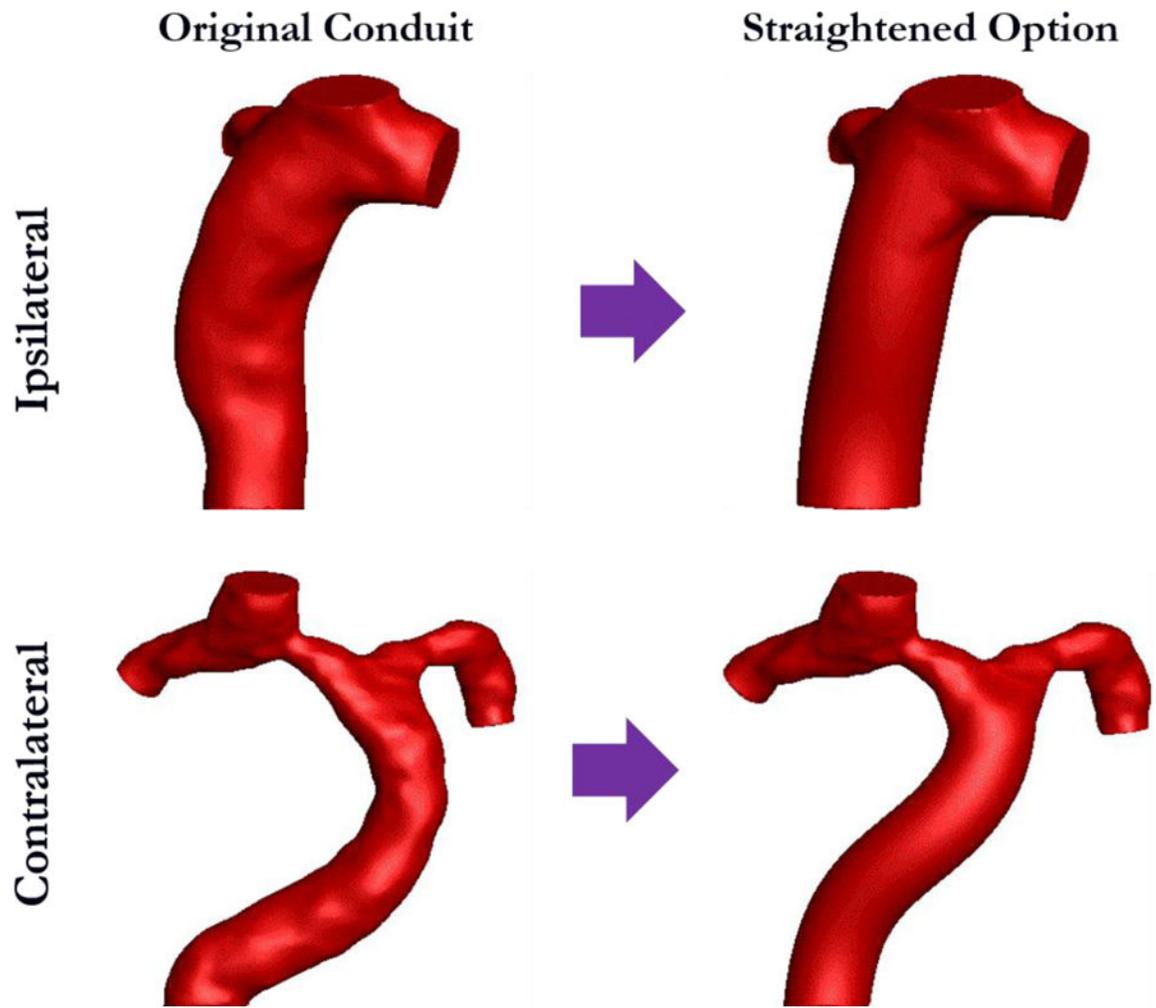
Contralateral

Figure 5.
Demonstration of virtual surgery for ipsilateral and contralateral conduits.
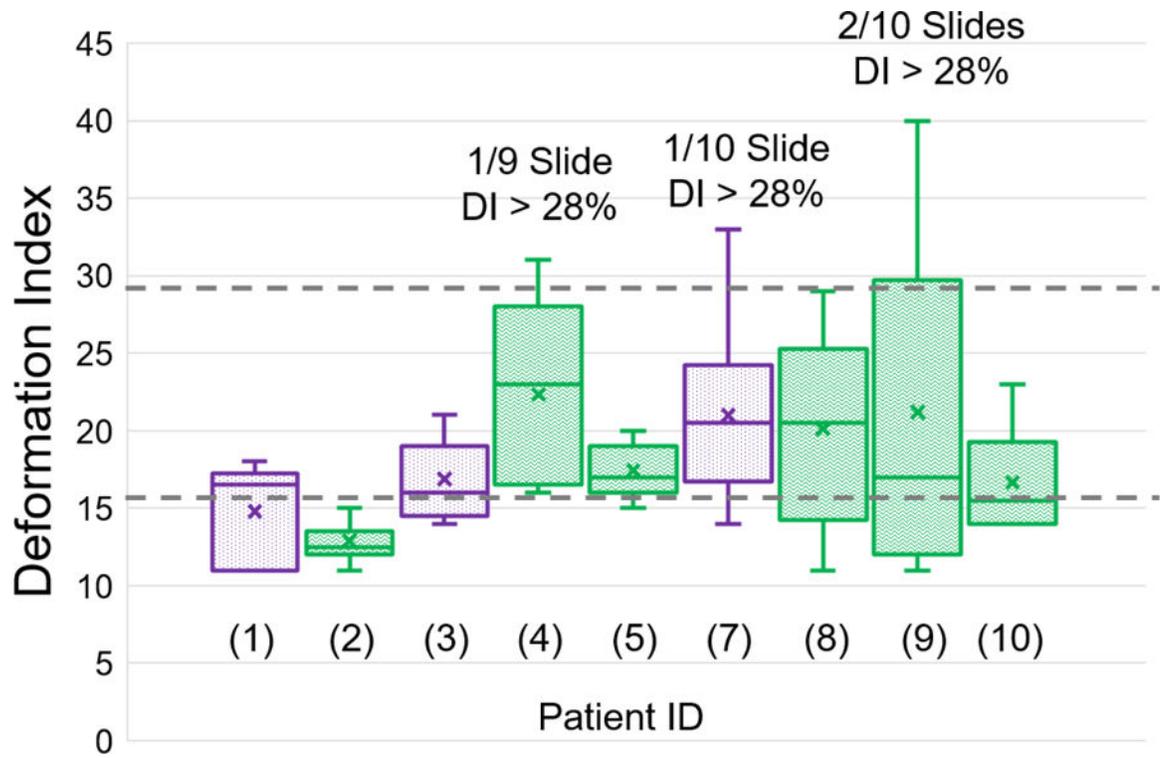
Figure 6.
DIs of all ACJ patients (green boxes: ipsilateral conduits; purple boxes: contralateral conduits). Two gray lines indicate the range of Dis for non-ACJ patients (16–28%)
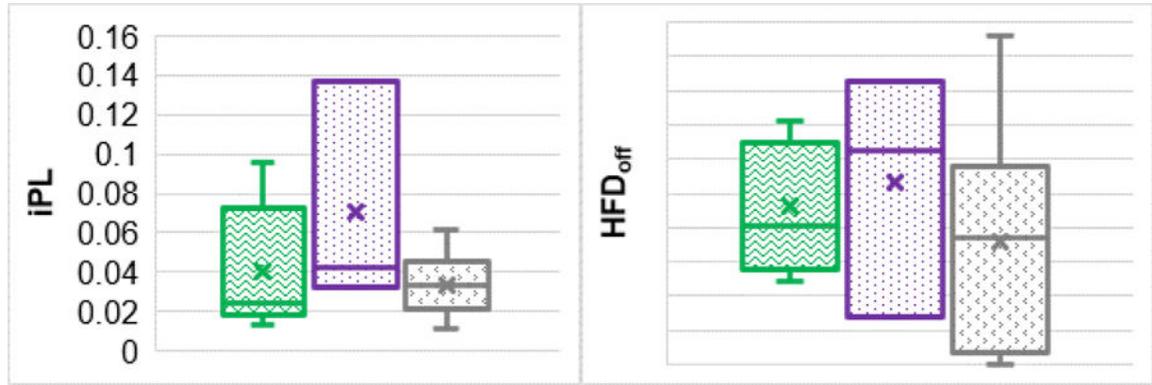
Figure 7.
Comparisons of iPL and HFD between patients with an ipsilateral conduit (green), patients with a contralateral conduit (purple), and non-ACJ patients with a regular Fontan conduit (gray).

Table 1

Patient Demographic Information and Clinical Characteristics

ID	Basic diagnosis	Age[1]/Sex	Preceding surgery	T[2]	IVC Side[3]	Conduit Type[4]	ConduitSize (mm)	CA[5]	T_{hosp}[6]
1	Situs ambiguous, Dx[a], Right isomerism, CAVCD[b], pulmonary atresia, supracardiac TAPVC[c]	12 / F	Left BDGS[l]	11	R	C	22	No	14
2	Situs solitus, Dx, DILV[d], restrictive BVF[e]	8 / F	Bilateral BDGS, SAM[m] resection	7	R	I	22	Yes	27
3	Situs ambiguous, Dx, DORV[f], SV[g], PS[h]	5 / F	Bilateral BDGS	4	R	C	18	No	17
4	Situs inversus, levocardia, CCTGA[i], PS	20 / F	Bilateral BDGS	9	L	I	20	No	16
5	Situs solitus, Dx, TA[j], VSD[k], PS	21 / F	Right BDGS	12	R	I	22	Yes	19
6	Situs solitus, Dx, CAVCD, SV, PS	5 / M	Bilateral BDGS	5	R	I	20	Yes	15
7	Situs solitus, Dx, CCTGA, VSD, PS	13 / M	AP[n] Shunt	13	R	C	20	Yes	14
8	Situs solitus, Dx, CCTGA, VSD, PS	6 / M	Right BDGS	6	R	I	20	Yes	13
9	Situs solitus, dextrocardia, TA, CCTGA, VSD, PS	7 / F	Right BDGS	5	R	I	20	Yes	17
10	Situs ambiguous, mesocardia, TA, DORV, VSD	14 / F	Bilateral BDGS	10	R	I	22	No	15

[1] Age: age at the time of the Fontan completion, in years

[2] T: time from previous surgery to Fontan, in years

[3] IVC Side: Left or Right inferior vena cava

[4] Conduit Type: Ipsilateral or Contralateral conduit

[5] CA: whether the patient underwent cardioplegic arrest, Yes/No

[6] T_{hosp}: hospitalization time, in days

[a] Dx: dextrocardia

[b] CAVCD: complete atrioventricular canal defect

[c] TAPVC: Total anomalous pulmonary venous connection

[d] DILV: double inlet left ventricle

[e] BVF: bulbo-ventricular foramen

[f] DORV: double outlet right ventricle

[g] SV: single ventricle

[h] PS: pulmonary atresia

[i]CCTGA: congenitally corrected transposition of the great arteries

[j]TA: tricuspid atresia

[k]VSD: ventricular septum defect

[l]BDGS: bidirectional Glenn shunt

[m]SAM: Subaortic membrane

[n]AP, atrio-pulmonary Fontan

Table 2

Clinical results for follow-up

ID	Follow up (years)	Issues on follow-up	Pulmonary vein compression?
1	6.2	None	None
2	6	Subaortic outflow obstruction	None
3	6.5	None	None
4	7	None	Mild on LLPV
5	5.5	Ectopic atrial tachycardia, on a beta blocker	None
6	5.3	None	Mild on RLPV
7	5.5	None	None
8	5.2	None	Mild on RLPV
9	6.5	None	Mild on RLPV
10	6	Supraventricular tachycardia, on a beta blocker	Mild on RLPV